

---

# A soil-water-balance approach to quantify groundwater recharge from irrigated cropland in the North China Plain

Eloise Kendy,<sup>1</sup> Pierre Gérard-Marchant,<sup>1</sup> M. Todd Walter,<sup>1</sup> Yongqiang Zhang,<sup>2</sup>  
Changming Liu<sup>2</sup> and Tammo S. Steenhuis<sup>1\*</sup>

<sup>1</sup> *Department of Biological and Environmental Engineering, Riley-Robb Hall, Cornell University, Ithaca, NY 14853, USA*

<sup>2</sup> *Laboratory of Land Hydrology and Water Resources, Institute of Geographic Sciences and Natural Resources Research, Chinese Academy of Sciences, Building 917, Datun Road, Anwai, Beijing 100101, China*

---

## Abstract:

Rapidly depleting unconfined aquifers are the primary source of water for irrigation on the North China Plain. Yet, despite its critical importance, groundwater recharge to the Plain remains an enigma. We introduce a one-dimensional soil-water-balance model to estimate precipitation- and irrigation-generated areal recharge from commonly available crop and soil characteristics and climate data. To limit input data needs and to simplify calculations, the model assumes that water flows vertically downward under a unit gradient; infiltration and evapotranspiration are separate, sequential processes; evapotranspiration is allocated to evaporation and transpiration as a function of leaf-area index and is limited by soil-moisture content; and evaporation and transpiration are distributed through the soil profile as exponential functions of soil and root depth, respectively. For calibration, model-calculated water contents of 11 soil-depth intervals from 0 to 200 cm were compared with measured water contents of loam soil at four sites in Luancheng County, Hebei Province, over 3 years (1998–2001). Each 50-m<sup>2</sup> site was identically cropped with winter wheat and summer maize, but received a different irrigation treatment. Average root mean-squared error between measured and model-calculated water content of the top 180 cm was 4.2 cm, or 9.3% of average total water content. In addition, model-calculated evapotranspiration compared well with that measured by a large-scale lysimeter. To test the model, 12 additional sites were simulated successfully. Model results demonstrate that drainage from the soil profile is not a constant fraction of precipitation and irrigation inputs, but rather the fraction increases as the inputs increase. Because this drainage recharges the underlying aquifer, improving irrigation efficiency by reducing seepage will not reverse water-table declines. Copyright © 2003 John Wiley & Sons, Ltd.

KEY WORDS recharge; water balance; soil moisture; infiltration; evapotranspiration; irrigation; drainage; North China Plain

## INTRODUCTION

The 320 000-km<sup>2</sup> North China Plain (Figure 1) is China's most important centre of agricultural production and home to more than 200 million people. In this nationally critical region, potential evapotranspiration greatly exceeds the annual precipitation of 500–800 mm. This water deficit is especially acute during the dry, windy spring planting season. For centuries, farmers accommodated the deficit by producing only two to three crops every 2 years (Yang, 1991). Since the advent of mechanized pumping wells in the 1960s, however, production has increased to two crops every year. As a result, the North China Plain now supplies more than 50% of the nation's wheat and 33% of its maize (State Statistics Bureau, 1999).

Alluvial aquifers underlying the North China Plain constitute the primary source of water for irrigation, as well as for urban and industrial use. In recent years, these competing demands have resulted in persistent, and in

---

\* Correspondence to: Tammo S. Steenhuis, Cornell University, Department of Biological and Environmental Engineering, 226 Riley-Robb Hall, Ithaca, NY 14853, USA. E-mail: tss1@cornell.edu

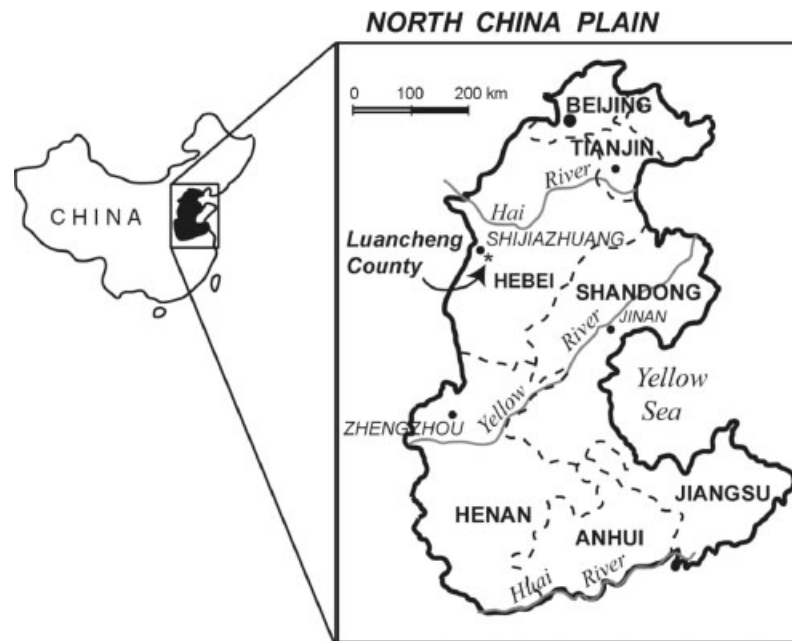


Figure 1. Location of Luancheng County and the North China Plain

some places very serious, water shortages (Xu and Peel, 1991; Yang, 1991). Groundwater levels are declining more than 1 m annually, stream flow has almost completely ceased, and in some places, land is subsiding irreversibly (Ministry of Water Resources Bureau, issued annually; Chen, 1992; Zhang and Zhang, 1995).

Currently, government officials are grappling with various management proposals to achieve sustainable groundwater withdrawal rates. However, their ability to make sound decisions is hampered by a lack of reliable information regarding the renewable quantity of the water resource. The alluvial aquifers potentially are recharged areally by precipitation and by seepage from irrigated fields, and laterally by mountain-front recharge. These mechanisms are particularly difficult to quantify in semi-arid settings such as the North China Plain (Gee and Hillel, 1988; Simmers, 1991; Stephens, 1993; Wood and Sanford, 1995; Scanlon *et al.*, 1997).

This study focuses on the areal component of recharge to unconfined aquifers in the North China Plain. Based on water-balance calculations, estimates of areal recharge to the North China Plain range from 2.6 billion m<sup>3</sup>/year according to the Ministry of Water Conservation (Liu and Wei, 1989) to 3.5 billion m<sup>3</sup>/year according to the Ministry of Geology (Liu and Wei, 1989) to more than 5 billion m<sup>3</sup>/year according to researchers Zhu and Zheng (1983). Although the details of these calculations are not available, a common approach is to assume that a certain fraction of precipitation and irrigation percolates to groundwater year after year, regardless of the quantity applied (e.g. Luancheng County Natural Resources Survey Team, 1979; Luancheng County Water Policy and Integrated Water Resources Management Office, 1993). Typically, this fraction, or infiltration coefficient, is obtained by simultaneously solving two equations for two unknowns—specific yield of the aquifer and infiltration coefficient—using two pairs of precipitation and water-level measurements. Often, methods in which recharge is determined as the residual component of groundwater-balance equations are inaccurate for semi-arid regions, where error margins in the other terms are large compared with the small amount of recharge (Gee and Hillel, 1988; Scanlon *et al.*, 1997). Although the groundwater-balance approach is straightforward, the large range of results confirms that the inherent uncertainty is significant. Moreover, both precipitation and irrigation in the North China Plain vary considerably from year to year, highlighting the need for a better approach for long-term analysis. Finally, water-level rises do not distinguish between areal and lateral inflow. This is especially important in the North

China Plain, where lateral inflow from the adjacent mountains is a significant, but also poorly quantified, source of groundwater recharge.

Clearly, an alternative method is needed for estimating areal recharge to the North China Plain. Approaches that have been used successfully elsewhere include inverse groundwater modelling, chemical tracers, solution of Richards' equation and 'tipping-bucket' models.

Inverse groundwater flow modelling is a variation on the water-balance method used specifically for estimating recharge (Stoertz and Bradbury, 1989). Inverse modelling has the advantages of requiring no information about the unsaturated zone and no assumptions regarding the mechanism of water movement through it. However, because all parameters are completely correlated, only their ratios can be estimated. Therefore, flow data—preferably stream baseflow—are essential for achieving a unique solution (Hill, 1998). Because groundwater no longer discharges to streams in the North China Plain, inverse modelling cannot yield reliable recharge estimates.

Chemical and isotopic tracers have been used successfully not only to help quantify recharge, but also to distinguish between sources (Allison *et al.*, 1994; Gee and Hillel, 1988; Wood and Sanford, 1995). However, tracer data are laborious and expensive to obtain, and thus far are not available for the North China Plain.

Many researchers have attempted to estimate groundwater recharge by solving Richards' equation for vertical water flow through the unsaturated zone. The functional relationships needed to apply Richards' equation, however, are time consuming and difficult to measure, especially at low water contents. Owing to their strategic national importance for agricultural production, basic characteristics have been determined for soils throughout the North China Plain; however, hydraulic conductivity functions and retention curves generally are not available.

Laboratory tests indicate that 'unsaturated hydraulic conductivity below the field capacity is so small that soil-water flow is usually assumed to be zero' (Burman and Pochop, 1994). To bypass onerous data requirements, then, one approach is to model infiltration as a storage-routing routine, in which only moisture in excess of field capacity moves downward in the soil profile (e.g. 'tipping bucket' module in Riha *et al.*, 1994). This effectively limits drainage simulation to the 1–3 day period following saturation. However, 'the redistribution process is in fact continuous' and 'can persist at an appreciable rate' for many days or even months after irrigation (Hillel, 1982). Therefore, although this approach has proven successful for wet regions, it does not adequately simulate semi-arid and arid conditions, where even the small quantity of subfield-capacity drainage is significant. This is clearly the case in the North China Plain, where soils continue to drain at moisture contents below field capacity throughout the winter, when precipitation is scant and irrigation has ceased.

Thus, although many methods have been developed for estimating areal recharge, none seems entirely appropriate both for the hydrogeological conditions unique to the North China Plain and for the limited data that are readily available. In this paper, we introduce a simple soil-water-balance model to estimate precipitation- and irrigation-generated areal recharge from easily accessible climate, soil and crop data. We then evaluate the model by comparing its results with field data obtained by Chinese Academy of Sciences researchers at Luancheng Agro-Ecological Research Station, located in Luancheng County, Hebei Province (Figure 1).

## THE MODEL

In order for a model to be useful, its data requirements must be readily obtainable. Daily precipitation and pan evaporation are measured by Meteorological Bureaus in or near every county in the North China Plain. Irrigation estimates are easy to obtain from farmers and agricultural researchers. Crop development has long been a major focus of research in China, and the literature contains ample information about the major crops grown in the North China Plain. Finally, basic soil characteristics, including porosity, wilting point, and permeability are available for all major agricultural soils. The model we developed determines areal recharge from these data.

The model does not simulate overland flow. In the North China Plain, groundwater pumping has depressed the water table to the extent that overland flow now occurs only when rainfall intensity exceeds surface soil permeability. If short-term precipitation data become available, then an overland flow routine can easily be added to the model, provided the time-step is shortened appropriately. In cases in which overland flow is known to occur, the current model provides an upper estimate of areal recharge.

Likewise, the model does not simulate snowmelt. Although winter temperatures dip below freezing on the North China Plain, precipitation during the winter is negligible.

The model simulates water movement through a soil profile consisting of any number of homogeneous layers, or soil horizons, on a daily basis. Ideally, each layer should be uniform, and the modelled profile should include the entire root zone. Because no analytical solution exists for the simultaneous calculation of complex infiltration and evapotranspiration patterns, many models use a finite-difference or finite-element approach to approximate these non-linear equations. Instead, we minimize computational effort by treating them as two separate, sequential processes, as successfully implemented by Kuo *et al.* (1999) and Zollweg *et al.* (1996).

Therefore, several processes are modelled during each time-step. First, precipitation or irrigation is added to the top layer, and then distributed downward in a simple ‘tipping bucket’ routine. Next, water is redistributed by solving for downward flux (infiltration) from each layer. Flux from the bottom layer may be considered groundwater recharge. Evapotranspiration from each layer is then determined. Evapotranspiration is separated into evaporation and transpiration, which is controlled by the crop-growth indicators, root depth, leaf-area index and soil-moisture content. Finally, the new soil-moisture content is calculated as the water-balance residual. The modelling procedure is described in detail below.

### *Infiltration*

In the model, each precipitation or irrigation application first is applied to the uppermost soil layer, which is allowed to fill to saturation. Water in excess of the layer’s effective porosity is distributed to successively deeper layers in a ‘tipping bucket’ fashion until each layer is filled to saturation or all of the water has been distributed. Any excess water that drains from the lowest layer becomes part of the groundwater recharge for that time-step.

Water in each layer is then redistributed downward as a function of hydraulic conductivity. To avoid relying upon the matric-potential functions required by Richards’ equation, we assume that gravity forces dominate over matric forces, and therefore a unit gradient exists throughout the soil profile. Thus, the modelled flux is always downward. Steenhuis *et al.* (1985) showed that these assumptions are reasonable, especially deep in the profile, where upward flux is insignificant. Because recharge depends more on evapotranspiration rates than on soil-water distribution, any errors introduced by these assumptions do not strongly influence recharge calculations.

Assuming no incoming or outgoing water flux other than that produced by unit gradient at the bottom of the layer, outflow from a layer can be expressed according to the conservation of mass as

$$L \frac{d\theta}{dt} = -K(\theta) \quad (1)$$

where  $L$  is layer thickness,  $\theta$  is the average volumetric soil-moisture content of the layer ( $L^3/L^3$  or  $L/L$ ),  $t$  is time (T) and  $K$  is unsaturated hydraulic conductivity ( $L/T$ ). Solving Equation (1) requires a function relating  $K$  to  $\theta$ . The function should involve few parameters, and those that are not readily available must be obtainable by calibration, using only existing data. Ideally, the function also should be relatively simple. To meet these standards, we assume an exponential relationship between  $K$  and  $\theta$  with dimensionless constant,  $\alpha$ , such that

$$K(\theta) = K_s \exp\left(-\alpha \frac{\theta_s - \theta}{\theta_s - \theta_d}\right) \quad (2)$$

where  $K_s$  is the saturated hydraulic conductivity,  $\theta_s$  is the volumetric moisture content of the soil layer at saturation, and  $\theta_d$  is the moisture content of dry soil. Steenhuis and van der Molen (1986) and Steenhuis *et al.* (1987) have used this exponential conductivity function successfully to estimate recharge in the north-eastern USA. It can be shown from data presented by Bresler *et al.* (1978) and Reichardt *et al.* (1972) that for homogeneous soils,  $\alpha$  is about 13. For heterogeneous soils,  $\alpha$  can be as large as 16 (Russo and Bresler, 1980). For modelling purposes,  $\alpha$  can be obtained by calibration. As  $\theta$  approaches  $\theta_d$ ,  $K(\theta)$  becomes very small but does not go to zero. Therefore, this equation is best limited to cases in which the soil does not become completely dry.

By substituting Equation (1) into Equation (2), assuming  $\theta_d = 0$ , separating variables, and integrating Equation (2), we obtain the volumetric moisture content of a single layer after infiltration

$$\theta_t = \theta_s - \frac{\theta_s}{\alpha} \ln \left[ \frac{\alpha K_s \Delta t}{L \theta_s} + \exp \frac{\alpha}{\theta_s} (\theta_s - \theta_{t-\Delta t}) \right] \quad (3)$$

The corresponding flux out of the layer is the difference between soil-water storage based on Equation (3) and that calculated at the start of the time-step. That flux is immediately added to the moisture content of the underlying layer. Discharge from the bottom layer drains into the aquifer, completing the calculation of groundwater recharge for one time-step.

*Total actual evapotranspiration*

Next, *actual* evapotranspiration,  $ET_a$  (L/T), from each layer is calculated and subtracted from soil-water storage.  $ET_a$  is a fraction of *potential* evapotranspiration,  $ET_p$ , which consists of potential evaporation from soil,  $E_p$ , and potential transpiration from plants,  $T_p$ . The ratio of  $E_p$  to  $T_p$  depends upon the development stage of the leaf canopy, expressed as  $\tau$ , the dimensionless fraction of incident beam radiation that penetrates the canopy (Campbell and Norman, 1998, p. 249)

$$\tau = \exp[(-K_b)(LAI)] \quad (4)$$

$K_b$  is the dimensionless canopy extinction coefficient, with a value of about 0.82 (Stockle, 1985) and  $LAI$  is leaf-area index ( $L^2/L^2$ ), daily values of which may be obtained from the literature for different crops (e.g. Hay and Walker, 1989; Fischer *et al.*, 2000) or calculated by crop-growth modelling (e.g. Riha *et al.*, 1994).

Accordingly,  $ET_p$  is allocated to

$$E_p = (\tau)(ET_p) \text{ and } T_p = (1 - \tau)(ET_p) \quad (5)$$

Actual evapotranspiration,  $ET_a$ , can be limited by the availability of water in the soil. Campbell and Norman (1998) derived a limiting function of  $U_p^* = 1 - 2\psi_s^*/3$  where  $U_p^*$  is dimensionless potential uptake rate and  $\psi_s^*$  is dimensionless soil-water potential. Assuming a relationship such that  $\theta_{fc}/\theta_s = (\psi_{fc}/\psi_e)^{-1/b}$  where the subscripts *fc* and *e* represent field capacity and air entry, respectively (Campbell and Norman, 1998), it can be shown that  $U_p^* = 1 - (\theta/\theta_{wp})^{-b}$ , where *wp* represents wilting point. The constant,  $b$ , is the inverse of the so-called pore-size distribution, or  $\lambda$  parameter, average values of which are presented by Rawls and Brakensiek (1985) and Maidment (1993, p. 5.14) for various soil textures. Thus, total actual evaporation and transpiration from the entire soil profile are modelled as

$$E_a = E_p \left[ 1 - \left( \frac{\theta}{\theta_{wp}} \right)^{-b} \right] \text{ and } T_a = T_p \left[ 1 - \left( \frac{\theta}{\theta_{wp}} \right)^{-b} \right] \quad (6)$$

where  $\theta$  is the calculated moisture content after infiltration (Equation 3) and  $b = 4$  (representing the entire soil profile, which is predominantly loam) for transpiration, and  $b = 0.3$  (representing the sandy, ploughed surface layer) for evaporation. Preliminary experiments at Luancheng Station indicate that evaporation may remove

water from as deep as 3 m in the soil profile, although most is removed from surficial layers. Transpiration removes water from all layers that contain plant roots. Water uptake,  $S$ , from a point,  $z$ , in a soil profile with an exponential root distribution can be expressed as (Novak, 1987)

$$S(z) = T_a \frac{\delta \exp \left[ -\delta \left( \frac{z}{z_r} \right) \right]}{z_r [1 - \exp(-\delta)]} \quad (7)$$

where  $z_r$  is the total root depth in the soil profile, and  $\delta$ , the water-use distribution parameter, is an empirical constant that determines the curvature of the exponential function, from almost linear ( $\delta$  approaching 0) to increasingly curved (Riha *et al.*, 1994). Values for most crops range from about 0.5 to 5.0; Novak (1987) reported a value of 3.64 for maize.

For a soil layer with roots extending from depth  $z_1$  to  $z_2$  from the land surface, the fraction of total  $T_a$  allocated to that layer can be obtained by integrating Equation (7) from  $z_1$  to  $z_2$

$$u_f^t = \left( \frac{1}{1 - \exp(-\delta)} \right) \left\{ \exp \left[ -\delta \left( \frac{z_1}{z_r} \right) \right] \left[ 1 - \exp \left( -\delta \frac{z_2 - z_1}{z_r} \right) \right] \right\} \quad (8)$$

where  $u_f^t$  represents the transpiration uptake fraction. The sum of  $u_f^t$  values over all layers in a soil profile is equal to 1.0. We use essentially the same equation for  $u_f^t$  to allocate evaporation to soil layers, substituting soil-layer depths for root depths. Because evaporation is more concentrated near the land surface than is transpiration,  $\delta$  for evaporation is about 10. Actual evaporation and transpiration from a single soil layer,  $i$ , during one time-step are

$$E_{a(i)} = u_f^t E_a \Delta t \text{ and } T_{a(i)} = u_f^t T_a \Delta t \quad (9)$$

To obtain the final moisture content,  $\theta_{i,t}$ , of layer  $i$  for time-step  $t$ ,  $E_a$  and  $T_a$  are subtracted from the soil-moisture content determined by Equation (3). At that point, all water-balance components have been determined and

$$\theta_{i,t} L_i = \theta_{i,t-1} L_i + q_{i-1,t} - q_{i,t} - E T_{a(i,t)} \quad (10)$$

where  $q$  is the flux between layers. If  $i = 1$ , then  $q_{i-1,t} = I_t + P_t$ , applied irrigation and precipitation.

To summarize and reiterate, several assumptions are inherent in the model. First, infiltration and evapotranspiration are separate, sequential processes. Second, gravity forces dominate over matric forces in the soil. Third, hydraulic conductivity,  $K$ , is an exponential function of soil-moisture content,  $\theta$  (Equation 2). Fourth, evapotranspiration is allocated to evaporation and transpiration as a function of  $LAI$  (Equation 5). Fifth, evapotranspiration is limited by soil-moisture content (Equations 6). Finally, evaporation and transpiration are distributed through the soil profile as exponential functions of soil and root depths, respectively (Equation 9).

The model code is written in Visual Basic and requires Microsoft Excel 2000 to run. Inputs to the model include daily precipitation, irrigation, potential evapotranspiration, leaf-area index and plant-root depth; and depth, effective porosity ( $\theta_{\text{sat}}$ ), wilting point ( $\theta_{\text{wp}}$ ), saturated hydraulic conductivity ( $K_s$ ) and  $\alpha$  of every user-defined soil layer. In addition, the user may specify a water-use distribution coefficient ( $\delta$ ). Outputs include daily actual evapotranspiration, groundwater recharge (drainage from the soil profile), and water content of each soil layer at the end of each time-step. The code can simulate several identical sites in one run, with each site receiving a different irrigation treatment. The model is initiated by specifying the starting soil-moisture content of each layer at each site. If initial moisture content is unknown, the simulation may begin at saturation immediately following a large precipitation or irrigation event. Alternatively, the modeller may begin by simulating 1 year of data repeatedly, until the annual soil-moisture change becomes negligible. The code loops first through the soil layers, then through the time-steps, and finally through the sites. A 3-year model of six sites runs in about 1 min on a 500 MHz computer with a Pentium (R) III processor and 256 MB of RAM; a 50-year model of one site takes 5–10 min.

## MODEL EVALUATION

*Field site description*

Field data collected at Luancheng Agro-Ecological Research Station (Chinese Academy of Sciences), Luancheng County, Hebei Province (Figure 1), from October 1998 through September 2001 provide input and targets for model calibration. The station is situated at an elevation of 50 m above mean sea-level, on nearly level ground. Average monthly temperatures range from about  $-4^{\circ}\text{C}$  in January to  $25^{\circ}\text{C}$  in July, with an average annual temperature of about  $15^{\circ}\text{C}$  and about 187 frost-free days annually. Most of the 461 mm of annual rainfall occurs during the humid summer months, with very little during spring and autumn, and even less during the cold, dry winters (Luancheng County Meteorological Bureau, unpublished data, 1971–2000). The Quaternary-age aquifer system underlying the station consists of laterally discontinuous layers of alluvium and reworked loess (Luancheng County Water Policy and Integrated Water Resources Management Office, 1993). Soils at the research station are characterized in Table I.

Climate data and plant-development indicators were measured at the field station. Precipitation was measured daily by summing hourly tipping-bucket measurements. Class A pan evaporation was measured daily. Root depths of winter wheat and maize were reported by Zhang (1999) as a function of the number of days since planting. Leaf-area index was measured by Zhang *et al.* (2002) and Wang *et al.* (2001).

Evapotranspiration and soil drainage were measured by a large-scale ( $7.5\text{ m}^3$ ) weighing lysimeter filled with undisturbed soil (Wang *et al.*, 2001). The lysimeter was weighed approximately daily 1 October 1998 through 12 January 2001. The lysimeter, which weighs about 2 t empty and about 14 t when full of soil, has a water-depth measurement precision of 0.02 mm (Zhang *et al.*, 2002). Although the measurements were precise, their accuracy was affected by the non-vegetated surroundings (the 'oasis effect'), which enabled vegetation in the lysimeter to transpire more than if surrounding plants had reduced wind advection (Burman and Pochop, 1994). Also, Zhang *et al.* (2002) noted that this effect may have been exacerbated by the lysimeter's metal and concrete frame, which extends above the soil surface and concentrates heat. Owing to the enhanced evapotranspiration, drainage from the lysimeter occurred only in July–August 2000.

Sixteen research sites were planted in winter wheat from October through June, and in maize from June through September, according to local cropping practices. Concrete curbs bound each  $50\text{-m}^2$  site to prevent runoff. Each site was well watered prior to the model-calibration period. Thereafter, the quantity and timing of irrigation applications varied between sites. Volumetric irrigation applications were measured directly. Each site was equipped with a neutron probe access tube in which soil-moisture content was measured approximately every 5 days at nine to ten depth intervals between 0 and 180 cm. Readings for 180–200 cm also were taken occasionally.

Table I. Characteristics of soil at Luancheng Station (X. Zhang, personal communication, 2001; Zhang and Yuan, 1994)

| Depth (cm) | Texture         | Bulk density ( $\text{g}/\text{cm}^3$ ) | Effective porosity (per cent by volume) | Field capacity (per cent by volume) | Wilting point (per cent by volume) | Saturated hydraulic conductivity (m/day) |
|------------|-----------------|---|---|-------------------------------------|------------------------------------|--|
| 0–25       | Loam            | 1.39                                    | 49                                      | 36                                  | 9.6                                | 1.1                                      |
| 25–40      | Loam            | 1.50                                    | 46                                      | 35                                  | 11.4                               | 0.43                                     |
| 40–60      | Loam            | 1.46                                    | 46                                      | 33                                  | 13.9                               | 0.73                                     |
| 60–85      | Loam            | 1.49                                    | 46                                      | 34                                  | 13.9                               | 0.71                                     |
| 85–120     | Silty clay loam | 1.54                                    | 46                                      | 34                                  | 12.9                               | 0.020                                    |
| 120–165    | Clay loam       | 1.63                                    | 42                                      | 39                                  | 13.9                               | 0.003                                    |
| 165–210    | Silty clay loam | 1.55                                    | 44                                      | 38                                  | 16.4                               | 0.016                                    |

### Model calibration

A model was set up to simulate 11 soil layers, with each layer corresponding to a measured soil-moisture interval. Four of the 16 neutron-probe sites were selected for model calibration; data from the remaining 12 were used to test the performance of the calibrated model. The calibration sites are: site 16, representing severely water-stressed conditions (4.0–12.0 cm/year irrigation); site 1, representing somewhat stressed conditions (21.0–32.8 cm/year), and sites 5 and 6, representing normal conditions (35.6–55.3 cm/year). Initial soil-moisture content was specified as measured on 1 October 1998.

Model calibration was accomplished primarily by trial-and-error adjustment of  $K_{\text{sat}}$  and  $\alpha$  to minimize root mean-squared error (RMSE) and optimize graphical fit between model-calculated and measured soil-moisture content of each layer (Figure 2) and of the total soil profile (Figure 3). In addition, model-calculated evapotranspiration was compared with that measured by lysimeter (Figure 4). Groundwater recharge, or drainage from the soil profile, was compared qualitatively with measured drainage from the lysimeter.

Table II lists the soil characteristics used in the calibrated model. Of these, model results are most sensitive to  $K_s$ . Initially, we input measured  $K_s$  (Table I). After calibration, values of  $K_s$  remained within one order of magnitude of the measured values. Although the modelled  $K_s$  of 0.1 m/day for 40–80 cm is less than the measured value of 0.7 m/day, the modelled value is consistent with the findings of Wang *et al.* (2001), who also simulated these layers at Luancheng Station as 0.1 m/day. We also decreased some of our modelled  $\theta_{\text{wp}}$  from those reported in Table I, in order to simulate the lower values of  $\theta$  measured during the simulation period. Average annual recharge calculated by the calibrated model differed from that calculated by the uncalibrated model (using measured soil characteristics and  $\alpha = 15$ ) by less than 10% for each of the four calibration sites.

Model input for daily  $ET_p$  was obtained by multiplying daily Class A pan evaporation by a pan coefficient of 0.7, which is a typical value under many conditions (Doorenbos and Pruitt, 1977). Daily pan evaporation was selected for model input—rather than monthly reference-crop  $ET$  (Allen *et al.*, 1998), which also was available—in order to capture the significant daily fluctuations evident in the pan data. Figure 5 shows that monthly values of  $0.7 \times$  pan evaporation closely represent monthly average reference-crop  $ET$  calculated according to the Penman-Monteith method, based on monthly average maximum and minimum daily temperature, relative humidity, wind speed and solar radiation (Smith *et al.*, 1998). A slightly lower pan coefficient would better match the Penman-Monteith values, but would result in less model-calculated  $ET_a$  and more model-calculated recharge.

Comparisons between model-calculated  $ET_a$  and direct measurements by the large-scale weighing lysimeter (Figure 4) indicate that the  $ET_p$  input are reasonable. Although it is thought that the lysimeter received roughly the same irrigation as sites 5 and 6, lysimeter irrigation was not recorded. Therefore, model-calculated and lysimeter-measured  $ET_a$  could not be compared directly. Nevertheless, the lysimeter data provide a useful benchmark for comparison. Because of the oasis effect discussed above, evapotranspiration from the lysimeter was expected to be somewhat greater than from sites 5 and 6. As expected, model-calculated  $ET_a$  from sites 5 and 6 were slightly less than that of the lysimeter (measured : modeled = 1.1; Figure 4). Sites 1 and 16, which received 65% and 24%, respectively, as much irrigation water as site 5, had correspondingly lower simulated  $ET_a$  (measured : modeled = 1.3 and 1.6; Figure 4) because less water was available for uptake.

Calibrated plant-growth indicators vary little from the reported measurements. Small adjustments were made to ensure that simulated roots were long enough to take up water from appropriate layers and that transpiration occurred throughout the entire growing season. Rather than change root depths from year to year to capture annual variation (evident in Figure 2, especially at depths of 140–160 cm), a single root-depth and LAI pattern was repeated each year. Sensitivity analyses during model calibration indicate that reasonable variations in LAI and root depth can be large enough to influence daily model-calculated  $ET_a$ , but annual recharge is not significantly affected.

Figures 2 and 3 compare measured to model-calculated soil-moisture contents and indicate RMSEs between the two. Overall, agreement between measured and modelled soil-moisture content is good. Average RMSE



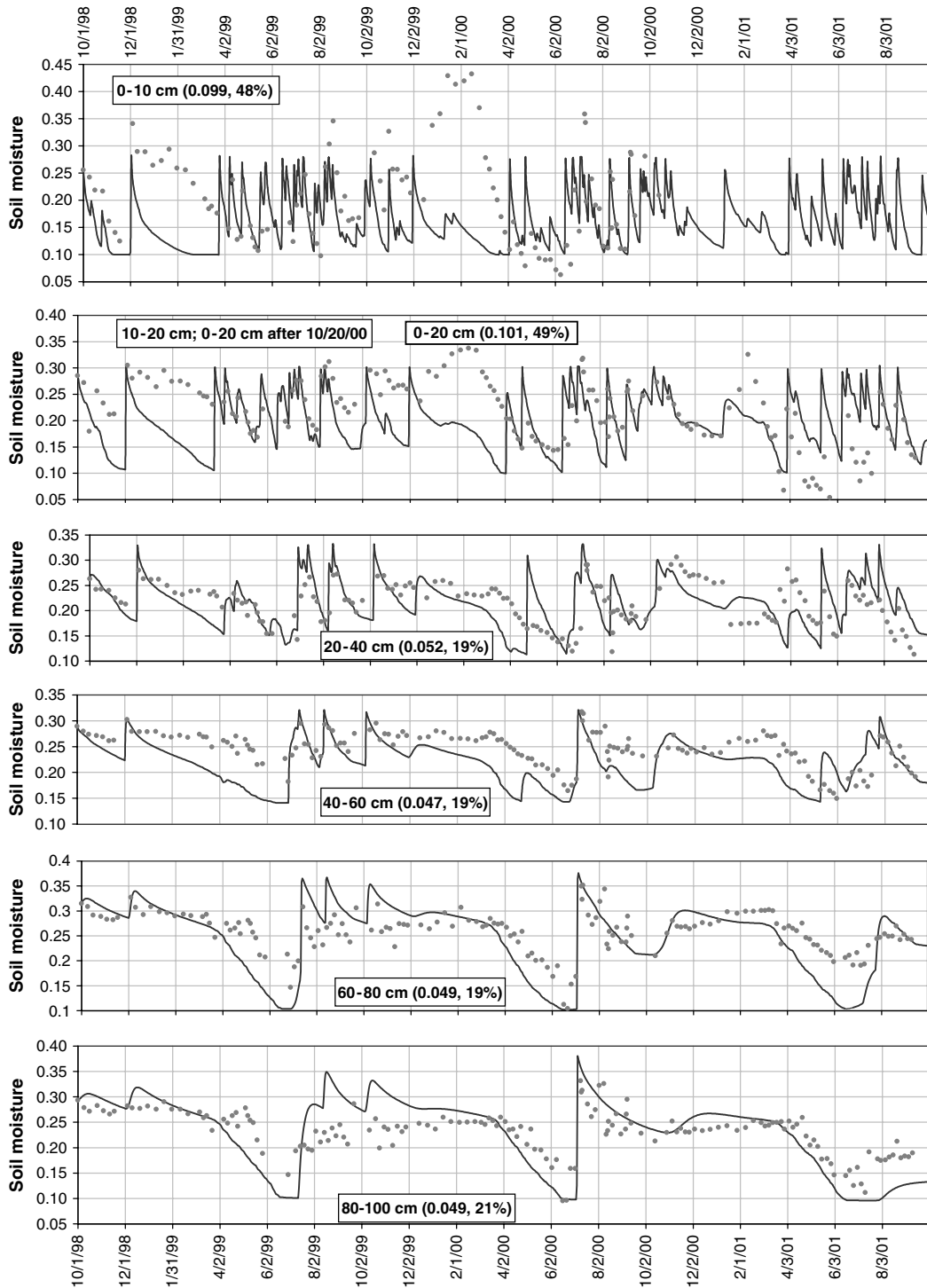


Figure 2. Comparison between measured (dots) and model-calculated (lines) volumetric soil-moisture content by layer at site 1. Layer depths from the land surface are indicated in boxes. Numbers in parentheses indicate root mean-squared error in cm/cm and as a percentage of average soil-moisture content. Precipitation and irrigation applications are shown in Figure 3

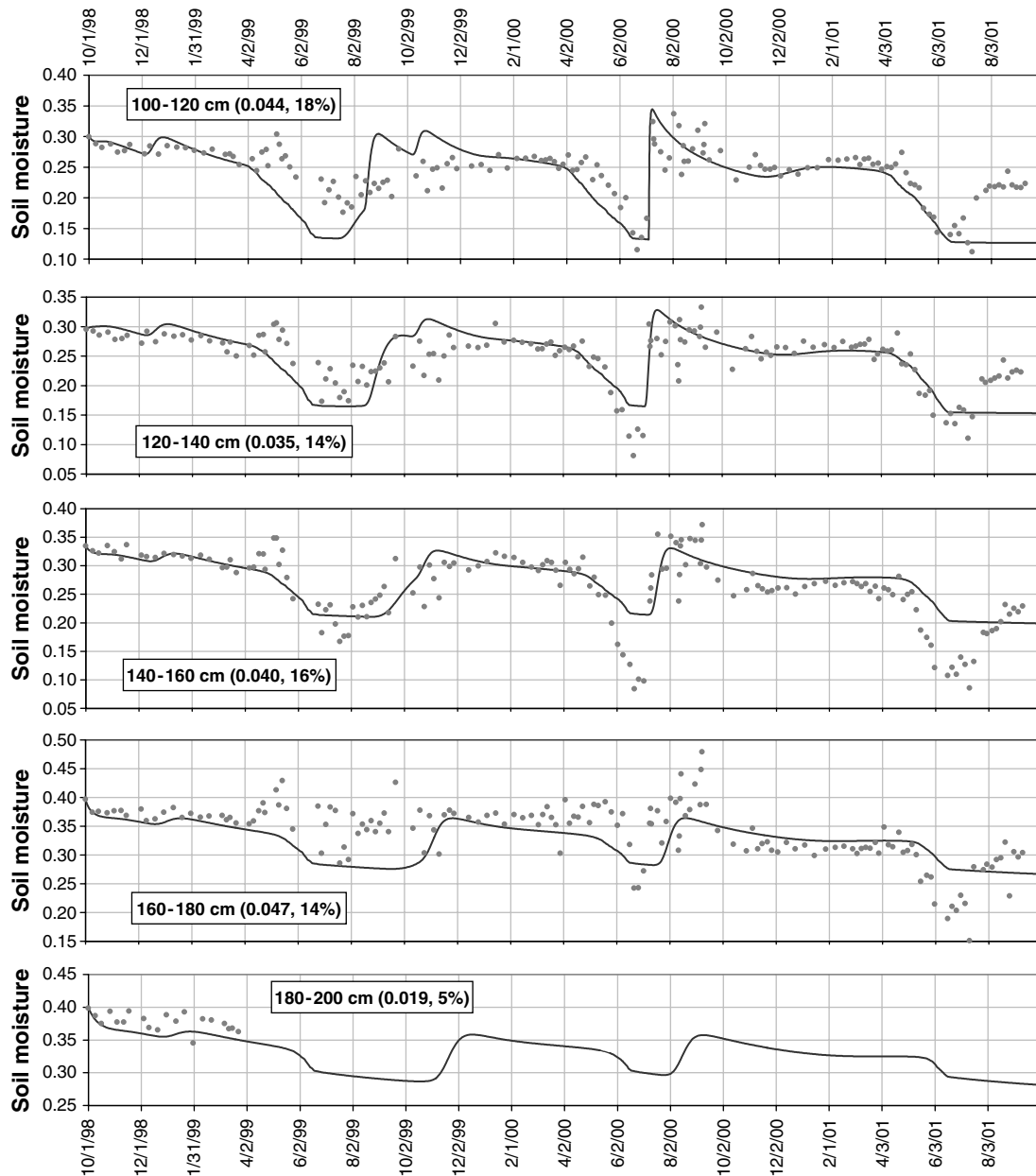


Figure 2. (Continued)

between measured and model-calculated water content of the top 180 cm was 4.2 cm, or 9.3% of average total water content (Figure 3). Soil-moisture content calculated by the model followed temporal trends of the measured data for most layers (Figure 2). An exception is the uppermost 20 cm, where neutron-probe readings are deemed unreliable owing to the interference of the air–soil interface (Gardner, 1986). During winter months, neutron-probe data indicated increasing soil-moisture content, despite a lack of precipitation. This phenomenon was particularly evident during winter 2000 at sites 1 and 5 (Figure 3). Because the apparent

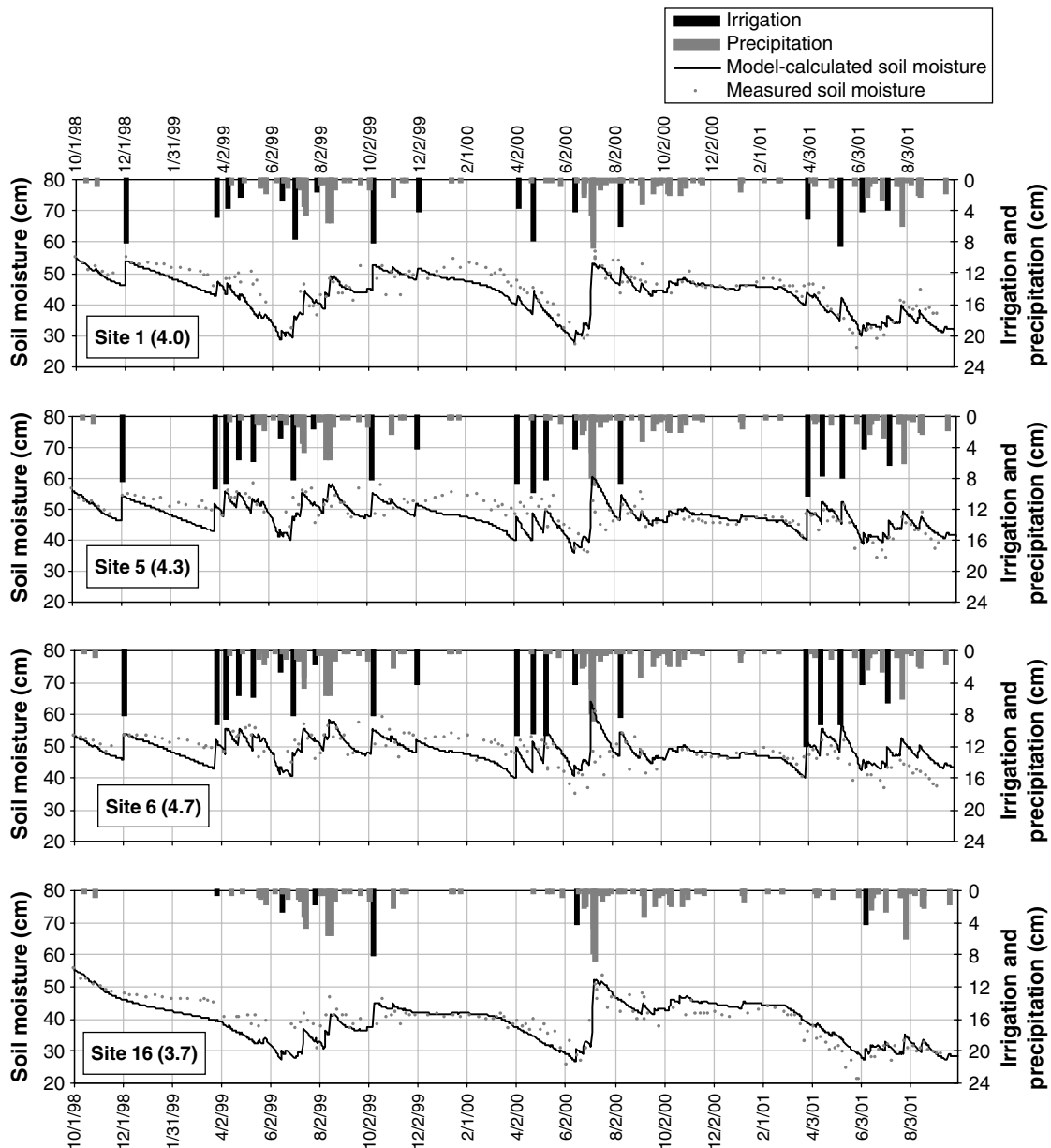


Figure 3. Comparison between measured and model-calculated moisture content of the top 180 cm of soil at four sites used for model calibration. Each site had a different irrigation treatment. Numbers in parentheses indicate root mean-squared error (cm)

moisture increase is most pronounced in the top 20 cm (Figure 2), it could be caused by misleading neutron-probe readings at the air–soil interface. Alternatively, there might have been some upward water movement, a process not simulated by the model owing to the unit-gradient assumption.

In general, the model does a somewhat better job of simulating the lower half of the soil-moisture profile than the upper half (Figure 2). However, it is drainage from the lower layers that controls groundwater recharge. Therefore, for determining recharge, this limitation is not a major concern.

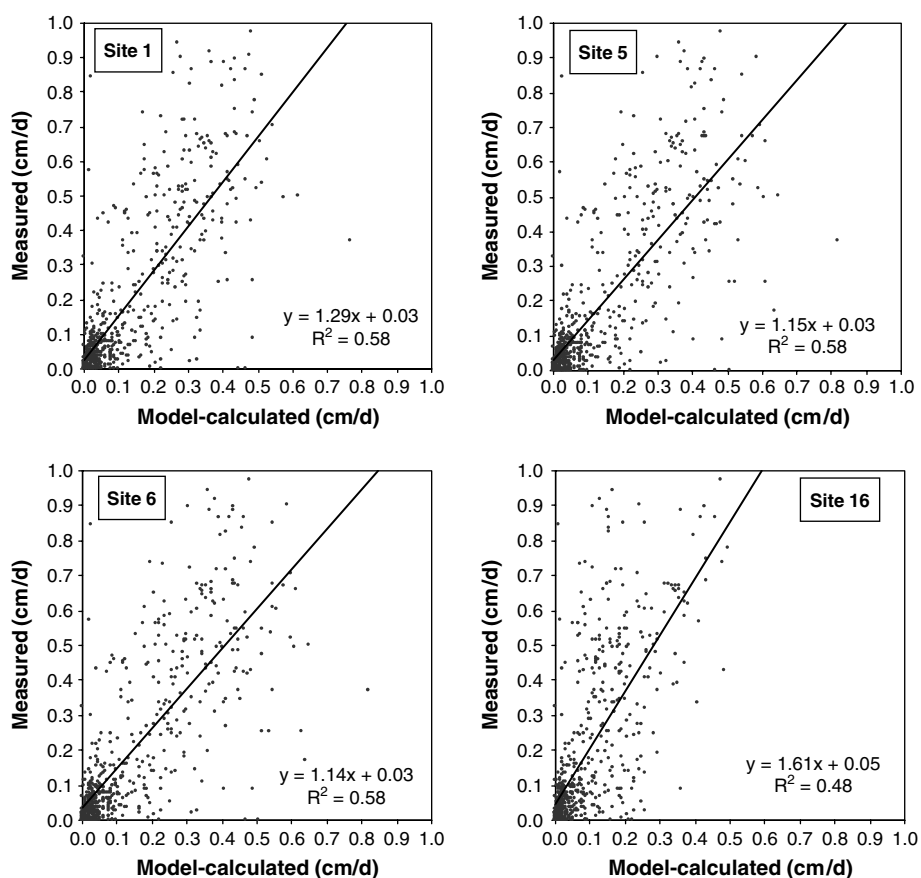


Figure 4. Comparison between lysimeter-measured and model-calculated daily evapotranspiration. Sites 5 and 6 received normal irrigation treatments (Figure 3); site 1 was somewhat water-stressed; site 16 was severely water-stressed. The lysimeter received irrigation treatments similar to sites 5 and 6. However, evapotranspiration from the lysimeter was influenced by the 'oasis effect'

Table II. Soil characteristics of the calibrated model

| Depth (cm) | Effective porosity, $\theta_{\text{sat}}$ (per cent by volume) | Wilting point, $\theta_{\text{wp}}$ (per cent by volume) | Saturated hydraulic conductivity, $K_s$ (m/day) | $\alpha$ |
|------------|--|--|---|----------|
| 0–10       | 49   | 10   | 1   | 13       |
| 10–20      | 49   | 10   | 1   | 15       |
| 20–40      | 46   | 11   | 0.4   | 15       |
| 40–60      | 40   | 14   | 0.1   | 15       |
| 60–80      | 46   | 10   | 0.1   | 16       |
| 80–100     | 46   | 9  | 0.06  | 13       |
| 100–120    | 44   | 11   | 0.06  | 13       |
| 120–140    | 42   | 7  | 0.03  | 13       |
| 140–160    | 40   | 4  | 0.01  | 13       |
| 160–180    | 44   | 16   | 0.01  | 15       |
| 180–200    | 44   | 16   | 0.01  | 15       |

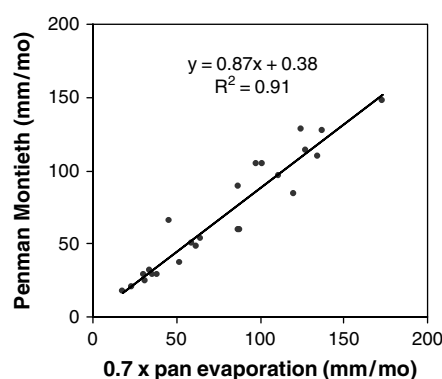


Figure 5. Comparison between monthly potential evapotranspiration calculated by the Penman–Monteith method and estimated as a fraction of Class A pan evaporation, 1998–2001

For most layers, differences between measured and modelled soil-moisture content were greatest immediately following large precipitation or irrigation events on dry soil, when actual water movement was faster than the model calculated. Apparently, preferential flow—a process not simulated by the model—is important during these periods. For example, in July 2000, drainage from the lysimeter peaked 6 days after a 3-day, 21-cm precipitation event. Model-calculated peak drainage from site 5 was delayed another 5 days, and the peak spread over a much longer period. Although most of this rapidly applied water eventually drained through the simulated profile, it probably was available for evapotranspiration for a longer period in the model than in the real world, resulting in slightly smaller recharge estimates than if these processes had been simulated accurately.

#### Model testing

After calibration, we tested the model by running it for the 12 remaining sites and comparing model-calculated to measured soil-moisture contents for 0–180 cm. The RMSEs for soil-moisture content (Figure 6) indicate little difference between the four sites used for calibration (average RMSE = 4.2, or 9.3% of average total water content) and the 12 sites used for testing (average RMSE = 4.8, or 11.9% of average total water content). The difference may be attributed in part to better screening of calibration-site data, which were scrutinized layer by layer. In contrast, outliers in the other 12 data sets were likely to be noticed only if they obviously affected the total moisture content of the entire profile.

The poor fit between measured and modeled soil-moisture content for sites 12 and 15 in year 2001 and for site 13 in years 2000 and 2001 (Figure 6) are difficult to explain. Sites 12, 13, 15 and 16 received identical irrigation treatments in 2001, yet measured  $\theta$  values varied significantly between sites for almost all layers. In contrast, model-calculated  $\theta$  values are, of course, identical. Likewise, sites 12 and 13 received identical irrigation in 2000, but only their modelled—not measured— $\theta$  values are the same. Possibly, actual soil characteristics of these sites differed from the others, reflecting the heterogeneity of the alluvial deposits from which they are derived. Soil-moisture content from 100 to 120 cm was particularly low at the outlier sites, suggesting the presence of laterally discontinuous sandy lenses.

## RESULTS AND DISCUSSION

Clearly, the model has both strong and weak points, which influence its application under various conditions. On the positive side, it provides a reliable, independent estimate of areal recharge based on relatively few, generally accessible data. In addition to recharge, the model also provides reasonable estimates of daily

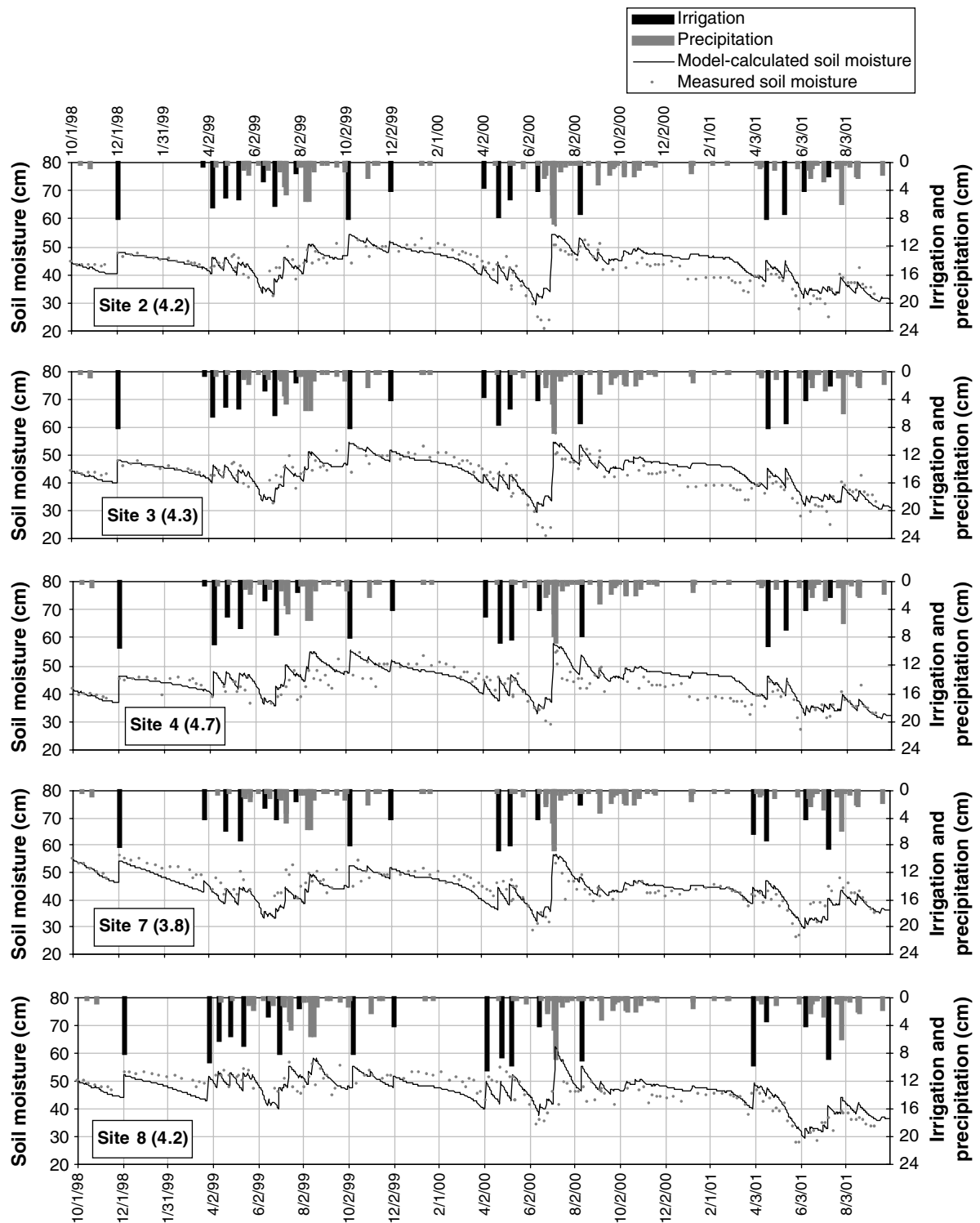


Figure 6. Comparison between measured and model-calculated moisture content of the top 180 cm of soil at 12 sites used for model evaluation. Each site had a different irrigation treatment. Numbers in parentheses indicate root mean-squared error (cm)

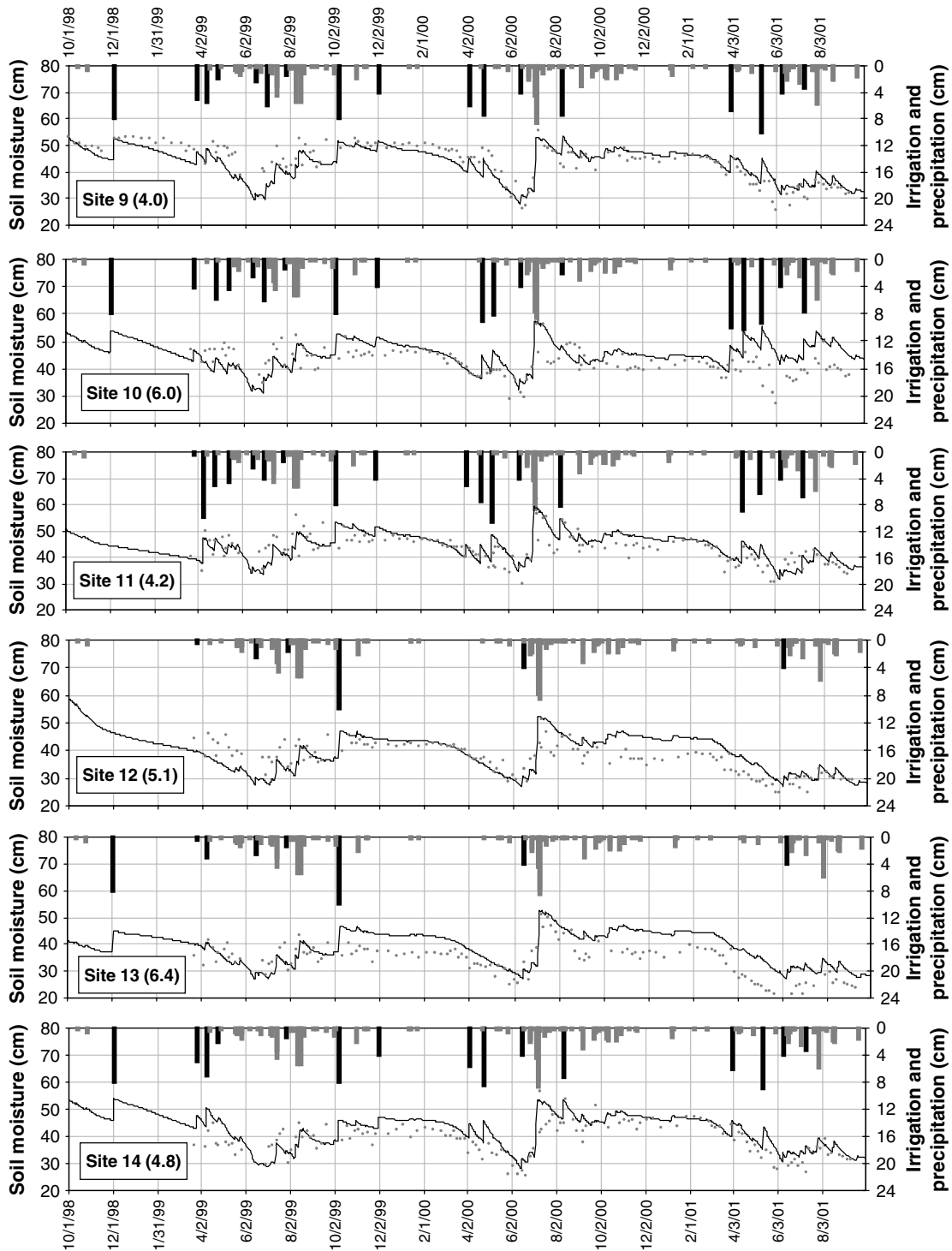


Figure 6. (Continued)

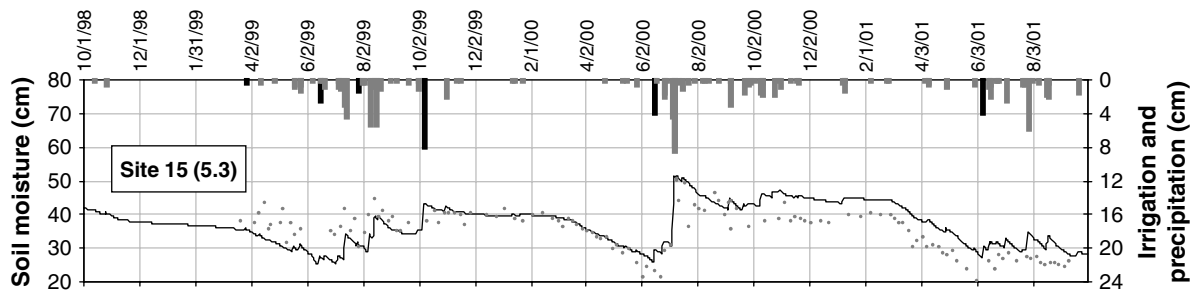


Figure 6. (Continued)

evapotranspiration. Although measured evapotranspiration data were not available to confirm this claim rigorously, reported groundwater pumping (Shijiazhuang Water Conservation Bureau, issued annually) and measured water table elevations beneath Luancheng Station support the water balance calculated by the model. That is, assuming a specific yield of 0.2, model-calculated recharge accounts for water table changes in 1998–99 and 2001, but underestimates the water table rise of 2000, which probably was boosted by lateral inflow from mountain runoff during that year's exceptionally wet monsoon season.

Compared with other simple soil-moisture models, this model better simulates drainage during prolonged periods between precipitation or irrigation events. To gauge the relative importance of soil-water redistribution that occurs when moisture content is less than field capacity, we modified the model so that infiltration would be zero unless soil-moisture content exceeds field capacity. Eliminating this subfield-capacity flow reduced simulated annual drainage from sites 5 and 6, the two normally irrigated sites, by 38–68%. Figure 7 shows how water-balance components varied over time at site 6 in the calibrated model. Precipitation and irrigation were input to the model; recharge and evapotranspiration were calculated. The delay between water application to the land surface and recharge is evident in the figure. Soil-moisture content is above field capacity only during the short periods immediately following precipitation and irrigation. However, the soil profile continues to drain, generating groundwater recharge, throughout the year.

The major weakness of the model is its relatively poor simulation of daily soil-moisture content. As is also the case for models based on Richards' equation, better characterization of soil properties,  $K_s$ ,  $\theta_{sat}$

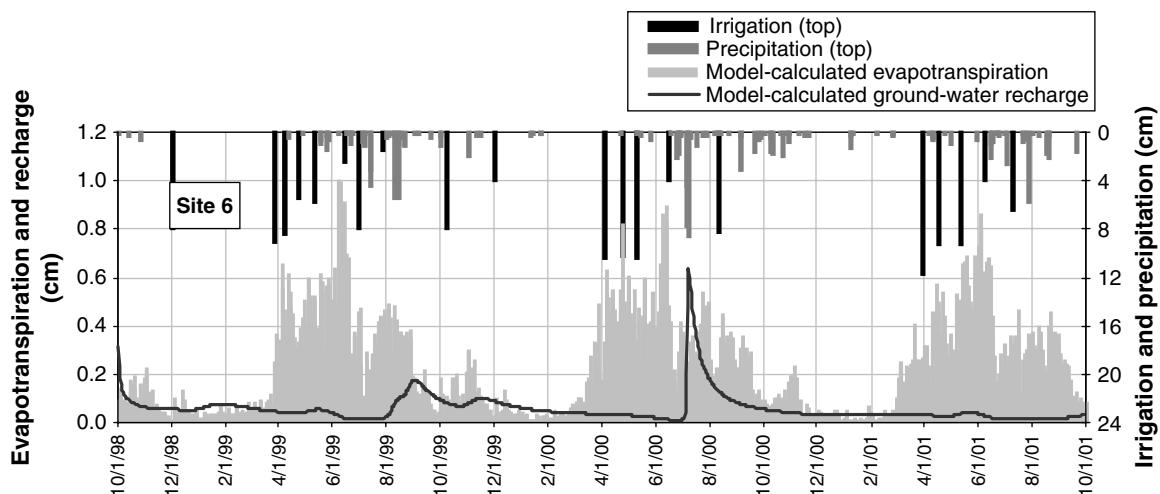


Figure 7. Model-calculated daily evapotranspiration and drainage (groundwater recharge) from site 6 with normal irrigation treatment, 1998–2001



Table III. Annual soil-water balances of all sites, 1998–2001. Years begin on 1 October and end on 30 September. Precipitation was 34.7 cm in 1998–99, 40.2 cm in 1999–2000 and 35.1 cm in 2000–2001. Precipitation and irrigation were measured; evapotranspiration, drainage (groundwater recharge) and soil-moisture changes were model-calculated. Each site was well watered prior to the calibration period

| Site number | Precipitation + irrigation (cm) |      |      | Actual evapotranspiration, $ET_a$ (cm) |      |      | Drainage (cm) |      |      | Soil-moisture change (cm) |      |      |         |      |      |         |      |      |         |      |      |       |       |       |       |       |       |
|-------------|---------------------------------|------|------|--|------|------|---------------|------|------|---------------------------|------|------|---------|------|------|---------|------|------|---------|------|------|-------|-------|-------|-------|-------|-------|
|             | 1998–99                         |      |      | 1999–00                                |      |      | 2000–01       |      |      | 1998–99                   |      |      | 1999–00 |      |      | 2000–01 |      |      | Average |      |      |       |       |       |       |       |       |
|             | 64.2                            | 73.0 | 79.8 | 56.1                                   | 73.0 | 79.8 | 81.6          | 59.7 | 60.6 | 62.8                      | 62.8 | 61.0 | 17.0    | 11.6 | 11.6 | 7.1     | 11.9 | 11.9 | 12.5    | 0.8  | 0.8  | 13.8  | 13.8  | 13.8  | 8.5   | 8.5   | 8.5   |
| 2           | 69.8                            | 79.8 | 79.8 | 56.1                                   | 79.8 | 79.8 | 68.6          | 62.5 | 64.9 | 63.6                      | 63.6 | 63.6 | 6.5     | 15.1 | 15.1 | 7.9     | 9.8  | 9.8  | 0.9     | -0.2 | -0.2 | -15.4 | -15.4 | -15.4 | -4.9  | -4.9  | -4.9  |
| 3           | 66.9                            | 73.0 | 73.0 | 57.3                                   | 73.0 | 73.0 | 65.7          | 62.9 | 59.7 | 63.4                      | 63.4 | 62.0 | 6.8     | 13.2 | 13.2 | 6.5     | 8.8  | 8.8  | -2.7    | 0.0  | 0.0  | -12.6 | -12.6 | -12.6 | -5.1  | -5.1  | -5.1  |
| 4           | 76.4                            | 85.5 | 85.5 | 57.1                                   | 73.0 | 73.0 | 73.0          | 63.6 | 67.0 | 63.9                      | 63.9 | 64.8 | 6.8     | 20.9 | 20.9 | 8.4     | 12.1 | 12.1 | 6.0     | -2.4 | -2.4 | -15.2 | -15.2 | -15.2 | -3.9  | -3.9  | -3.9  |
| 5           | 83.4                            | 90.6 | 90.6 | 70.7                                   | 81.6 | 81.6 | 81.6          | 66.1 | 68.7 | 68.0                      | 68.0 | 67.6 | 25.7    | 23.9 | 23.9 | 9.1     | 19.5 | 19.5 | -8.4    | -1.9 | -1.9 | -6.3  | -6.3  | -6.3  | -5.5  | -5.5  | -5.5  |
| 6           | 83.4                            | 95.5 | 95.5 | 75.7                                   | 84.9 | 84.9 | 84.9          | 66.3 | 69.0 | 68.1                      | 68.1 | 67.8 | 23.3    | 28.6 | 28.6 | 10.9    | 20.9 | 20.9 | -6.2    | -2.1 | -2.1 | -3.2  | -3.2  | -3.2  | -3.9  | -3.9  | -3.9  |
| 7           | 67.9                            | 74.5 | 74.5 | 60.9                                   | 67.8 | 67.8 | 67.8          | 63.2 | 59.8 | 62.9                      | 62.9 | 62.0 | 16.5    | 15.3 | 15.3 | 6.5     | 12.8 | 12.8 | -11.8   | -0.6 | -0.6 | -8.5  | -8.5  | -8.5  | -7.0  | -7.0  | -7.0  |
| 8           | 82.0                            | 93.6 | 93.6 | 60.5                                   | 78.7 | 78.7 | 78.7          | 65.9 | 69.0 | 62.9                      | 62.9 | 65.9 | 18.4    | 26.1 | 26.1 | 9.4     | 18.0 | 18.0 | -2.2    | -1.5 | -1.5 | -11.9 | -11.9 | -11.9 | -5.2  | -5.2  | -5.2  |
| 9           | 65.3                            | 77.0 | 77.0 | 59.1                                   | 67.2 | 67.2 | 67.2          | 61.7 | 63.2 | 65.2                      | 65.2 | 63.4 | 14.8    | 10.8 | 10.8 | 8.1     | 11.2 | 11.2 | -11.2   | 3.0  | 3.0  | -14.3 | -14.3 | -14.3 | -7.5  | -7.5  | -7.5  |
| 10          | 67.2                            | 75.5 | 75.5 | 76.5                                   | 73.1 | 73.1 | 73.1          | 62.5 | 60.2 | 67.9                      | 67.9 | 63.6 | 15.4    | 16.0 | 16.0 | 8.1     | 13.2 | 13.2 | -2.2    | -0.8 | -0.8 | 0.5   | 0.5   | 0.5   | -3.7  | -3.7  | -3.7  |
| 11          | 62.9                            | 87.6 | 87.6 | 61.1                                   | 70.5 | 70.5 | 70.5          | 60.4 | 67.3 | 63.9                      | 63.9 | 63.9 | 10.7    | 18.2 | 18.2 | 8.7     | 12.5 | 12.5 | -8.2    | 2.1  | 2.1  | -11.5 | -11.5 | -11.5 | -5.9  | -5.9  | -5.9  |
| 12          | 39.2                            | 54.2 | 54.2 | 39.1                                   | 44.2 | 44.2 | 44.2          | 45.6 | 42.3 | 48.8                      | 48.8 | 45.6 | 17.7    | 5.0  | 5.0  | 6.5     | 9.7  | 9.7  | -24.1   | 6.9  | 6.9  | -16.2 | -16.2 | -16.2 | -11.1 | -11.1 | -11.1 |
| 13          | 50.2                            | 54.2 | 54.2 | 39.1                                   | 47.8 | 47.8 | 47.8          | 51.6 | 42.3 | 48.8                      | 48.8 | 47.6 | 5.4     | 4.4  | 4.4  | 6.5     | 5.4  | 5.4  | -6.9    | 7.5  | 7.5  | -16.2 | -16.2 | -16.2 | -5.2  | -5.2  | -5.2  |
| 14          | 58.2                            | 77.5 | 77.5 | 57.7                                   | 64.5 | 64.5 | 64.5          | 60.3 | 63.6 | 64.5                      | 64.5 | 62.8 | 15.4    | 5.5  | 5.5  | 8.0     | 9.7  | 9.7  | -17.5   | 8.3  | 8.3  | -14.8 | -14.8 | -14.8 | -8.0  | -8.0  | -8.0  |
| 15          | 39.2                            | 52.2 | 52.2 | 39.1                                   | 43.5 | 43.5 | 43.5          | 44.5 | 42.2 | 48.8                      | 48.8 | 45.2 | 3.8     | 0.9  | 0.9  | 6.0     | 3.6  | 3.6  | -9.1    | 9.1  | 9.1  | -15.8 | -15.8 | -15.8 | -5.3  | -5.3  | -5.3  |
| 16          | 39.2                            | 52.2 | 52.2 | 39.1                                   | 43.5 | 43.5 | 43.5          | 45.5 | 42.3 | 48.8                      | 48.8 | 45.5 | 14.0    | 3.0  | 3.0  | 6.5     | 7.8  | 7.8  | -20.2   | 6.9  | 6.9  | -16.2 | -16.2 | -16.2 | -9.8  | -9.8  | -9.8  |

and  $\theta_{wp}$ , would improve these calculations. However, detailed characterization is especially difficult in the heterogeneous alluvial settings for which the model otherwise is most suited. Thus, use of model results would best be restricted to the seasonal or annual estimates of recharge and evapotranspiration needed for long-term water management.

The major findings of the Luancheng Station simulations are that areal recharge does occur; its timing depends on the temporal distribution of water inputs; and its magnitude depends not only on precipitation and irrigation, but also on evapotranspiration. Figure 7 indicates the importance of temporal distribution of precipitation and irrigation in generating recharge. That is, antecedent moisture conditions and the time period over which rain falls are more important than the total quantity of rainfall. Therefore, intense rains of the summer monsoon generated more recharge than did the sum of smaller precipitation events and irrigation applications during the rest of the year.

Model-calculated magnitudes of annual recharge are shown in Table III, which tallies calculated annual water balances of all 16 sites. Because all sites were well watered prior to the calibration period (on 25 September 1998), average annual soil-moisture changes were negative. Although all sites except 5 and 6 were subjected to some degree of water stress,  $ET_a$  varied little between sites, except for the extremely water-stressed sites, 12, 13, 15 and 16. For healthy crops under normal conditions, this leads to the hypothesis that drainage from the soil profile is not a simple fraction of precipitation and irrigation, as commonly assumed. Rather, drainage estimates also must consider  $ET_a$ .

To test this hypothesis, we set up a model run to simulate the same climate and wheat/maize-cropping pattern as for site 6 in 1999–2000, but with irrigation applications ranging from 0.35 to 1.5 times that applied in 1999–2000. Results are plotted in Figure 8, which shows that recharge is better predicted as a linear function of precipitation ( $P$ ), irrigation ( $I$ ) and  $ET_a$  ( $r^2 = 0.92$ ) than simply as a constant fraction of  $P + I$  ( $r^2 = 0.56$ ). As  $P + I$  decrease to the extent that the crops become water-stressed,  $ET_a$  begins to decrease as well, and the linear relationship no longer holds. At low  $P + I$ , a power function better predicts recharge (Figure 8). In general, the smaller the inputs, the smaller is the fraction that drains from the soil profile. Because this drainage recharges the underlying aquifer, improving irrigation efficiency by reducing seepage will not reduce groundwater declines. Hence, the great deal of effort expended in recent years to line irrigation ditches in the hope of saving water would better have been spent finding ways to reduce evapotranspiration.

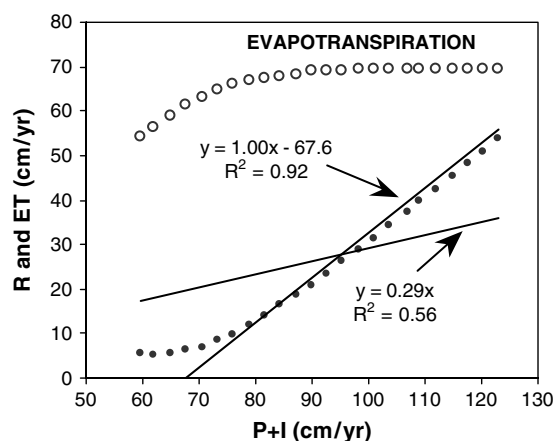


Figure 8. Relationship between model-calculated annual recharge ( $R$ ), evapotranspiration ( $ET$ ), and precipitation plus irrigation ( $P + I$ ) for a typical wheat/maize-cropping pattern receiving irrigation applications ranging from 0.3 to 1.5 times that applied to site 6 in 1999–2000, when the model-calculated evapotranspiration was 67.6 cm/year. Lines show best-fit linear functions with intercepts of 67.6 and 0.0

## CONCLUSION

The model presented in this paper can be a useful tool for estimating areal groundwater recharge under a wide variety of circumstances. It is particularly suitable to areas with little topographic relief, relatively deep water tables, and insignificant snowmelt, and where available data are limited to the basic climate, soil and crop information typical of major agricultural areas. In addition to the North China Plain, this includes large areas of India, Pakistan and the Arabian Peninsula, where excessive groundwater pumping also is a serious concern.

In areas such as these, groundwater modelling is an important tool for quantifying the groundwater balance—an essential prerequisite for sound, scientific groundwater management. However, such models are of limited value when both areal and lateral recharge are poorly quantified. By generating an independent estimate of areal recharge, the soil-water balance model presented in this paper also provides an important constraint on estimates of lateral recharge needed for groundwater modelling.

Owing to the discrepancy between the hourly to daily time-scale of unsaturated flow and the monthly to yearly time-scale of groundwater flow, it is not feasible to simulate both systems accurately in one groundwater model (Anderson and Woessner, 1992). As an alternative, Frind and Verge (1978) advocate linking a one-dimensional unsaturated-zone model to a two- or three-dimensional groundwater model. In the absence of extensive field data, the one-dimensional unsaturated-zone model described in this paper provides a viable alternative to Richards' equation-based approaches for calculating drainage through a soil profile. With its simple spreadsheet format and easily accessible input requirements, this model can readily generate the recharge input needed for groundwater modelling, and ultimately for well-informed, fully integrated water management of the North China Plain.

## ACKNOWLEDGEMENTS

Funding for this research was generously provided through an assistantship provided by the US Department of Education and by grants from the Cornell University East Asia Program, Cornell International Institute for Food, Agriculture, and Development Travel Grant; the Teresa Heinz Scholars for Environmental Research; and the International Water Management Institute. Soil-moisture observations were supported by a basic research grant from the National Natural Science Fund of China (No.49890330). Yanjun Shen and Jia Jinsheng helped collect field data. Special appreciation is extended to Susan J. Riha and Zhang Xiying for many helpful discussions contributing to the development of the model. Finally, many thanks to Weston Dripps and Gerrit H. de Rooij for their insightful reviews of this paper.

## REFERENCES

- Allen RG, Pereira LS, Raes D, Smith M. 1998. *Crop Evapotranspiration—Guidelines for Computing Crop Water Requirements*. FAO Irrigation and Drainage Paper 56, Food and Agriculture Organization of the United Nations: Rome; 300 pp.
- Allison GB, Gee GW, Tyler SW. 1994. Vadose-zone techniques for estimating groundwater recharge in arid and semiarid regions. *Soil Science Society of America Journal* **58**(1): 6–14.
- Anderson MP, Woessner WW. 1992. *Applied Groundwater Modeling: Simulation of Flow and Advective Transport*. Academic Press: San Diego; 381 pp.
- Bresler E, Russo D, Miller RD. 1978. Rapid estimate of unsaturated hydraulic conductivity function. *Soil Science Society of America Journal* **42**(1): 170–172.
- Burman R, Pochop LO. 1994. *Evaporation, Evapotranspiration, and Climatic Data*. Elsevier: Amsterdam; 278 pp.
- Campbell GS, Norman JM. 1998. *An Introduction to Environmental Biophysics*, 2nd edn. Springer-Verlag: New York; 286 pp.
- Chen Z. 1992. Water resources development in China. In *Country Experiences with Water Resources Management—Economic, Institutional, Technological and Environmental Issues*, Le Moigne G, Barshouti S, Feder G, Garbus L, Xie M (eds). Technical Paper 175, World Bank: Washington, DC; 175–181.
- Doorenbos J, Pruitt WO. 1977. *Guidelines for Predicting Crop Water Requirements*. FAO Irrigation and Drainage Paper **24**, 2nd Ed; Food and Agriculture Organization of the United Nations: Rome.
- Fischer G, van Velthuisen H, Nachtergaele F, Meadow S. 2000. *Global Agro-Ecological Zones, Appendix VII—Parameters for Biomass and Yield Calculations*. Food and Agriculture Organization of the United Nations: Rome and International Institute for Applied Systems Analysis: Laxenburg, Austria. [Accessed on 11 April 2002 from URL <http://www.fao.org/ag/agl/agll/gaez/index.htm>]

- Frind EO, Verge MJ. 1978. Three-dimensional modeling of groundwater flow systems. *Water Resources Research* **14**(5): 844–856.
- Gardner WH. 1986. Water Content. In *Methods of Soil Analysis, Part 1: Physical and Mineralogical Methods*, 2nd Edn, Klute A (ed.). American Society of Agronomy, and Soil Science Society of America: Madison, WI; 493–544.
- Gee GW, Hillel D. 1988. Groundwater recharge in arid regions: review and critique of estimation methods. *Hydrological Processes* **2**(3): 255–266.
- Hay RKM, Walker AJ. 1989. *An Introduction to the Physiology of Crop Yield*. Longman Scientific & Technical: Harlow; 292 pp.
- Hill M. 1998. Methods and guidelines for effective model calibration. *U.S. Geological Survey Water-resources Investigation Report* **98-4005**: 90 pp.
- Hillel D. 1982. *Introduction to Soil Physics*. Academic Press: San Diego; 364 pp.
- Kuo W-L, Steenhuis TS, McCulloch CE, Mohler CL, Weinstein DA, DeGloria SD, Swaney DP. 1999. Effect of grid size on runoff and soil moisture for a variable-source-area hydrology model. *Water Resources Research* **35**(11): 3419–3428.
- Liu C, Wei Z. 1989. *Agricultural Hydrology and Water Resources of the North China Plain*. Science Press: Beijing; 236 pp. (In Chinese.)
- Luancheng County Natural Resources Survey Team. 1979. *Luancheng County Agriculture and Natural Resources Investigation and Agricultural Zoning Report (Luancheng Xian Nongye Ziran Ziyuan Diaocha he Nongye Quhua Baogao)*. Chinese Academy of Sciences: Luancheng County, Hebei Province; 6 Vols.
- Luancheng County Water Policy and Integrated Water Resources Management Office. 1993. *Investigation Report on Current Development and Use of Water Resources (Shuiziyuan Kaifa Liyong Xianzhuang Diaocha Baogao)*. Shijiazhuang City, Luancheng County, Hebei Province.
- Maidment DR. 1993. *Handbook of Hydrology*. McGraw-Hill: New York.
- Ministry of Water Resources Bureau. Issued annually. *China Water Resources Bulletin*. (In Chinese.)
- Novak V. 1987. Estimation of soil-water extraction patterns by roots. *Agricultural Water Management* **12**(4): 271–278.
- Rawls WJ, Brakensiek DL. 1985. Prediction of soil water properties for hydrologic modeling. In *Watershed Management in the Eighties*. American Society of Civil Engineers: Reston, VA; 293–299.
- Reichardt K, Nielsen DR, Biggar JW. 1972. Scaling of horizontal infiltration into homogeneous soils. *Soil Science Society of America Proceedings* **36**(2): 241–245.
- Riha SJ, Rossiter DG, Simoens P. 1994. *GAPS General-Purpose Atmosphere-Plant-Soil Simulator Version 3-0 User's Manual*. Department of Soils, Crops and Atmospheric Sciences, Cornell University: Ithaca, NY. [Accessed on 1 September 2002 from URL <http://www.css.cornell.edu/faculty/sjr4/gaps.html>]
- Russo D, Bresler E. 1980. Scaling soil hydraulic properties of a heterogeneous field soil. *Soil Science of America Journal* **44**(4): 681–684.
- Scanlon BR, Tyler SW, Wierenga PJ. 1997. Hydrologic issues in arid, unsaturated systems and implications for contaminant transport. *Reviews of Geophysics* **35**(4): 461–490.
- Shijiazhuang Water Conservation Bureau. Issued annually. Basic water conservation and construction data for Shijiazhuang Prefecture. (In Chinese.)
- Simmers I. 1991. Natural groundwater recharge estimation in (semi)arid zones—some state-of-the-art observations. In *The State-of-the-Art of Hydrology and Hydrogeology in the Arid and Semi-Arid Areas of Africa*, Stout GE, Demissie M (eds). Proceedings of the Sahel Forum, 1989, UNESCO: Ouagadougou, Burkina Faso; 373–386.
- Smith M, Clarke D, El-Askari K. 1998. *CropWat 4 Windows*. Food and Agriculture Organization of the United Nations: Rome. [Accessed on 1 September 2002 from URL <http://www.fao.org/ag/agl/aglw/cropwat.htm>]
- State Statistics Bureau. 1999. *Statistics Yearbook of China*. Statistics Publishing House: Beijing.
- Steenhuis TS, van der Molen WH. 1986. The Thornthwaite–Mather procedure as a simple engineering method to predict recharge. *Journal of Hydrology* **84**(3–4): 221–229.
- Steenhuis TS, Jackson C, Kung K-JS, Brutsaert WH. 1985. Measurement of groundwater recharge on eastern Long Island. *Journal of Hydrology* **79**(1–2): 145–169.
- Steenhuis TS, Pacenka S, Porter KS. 1987. MOUSE: a management model for evaluating groundwater contamination from diffuse surface sources aided by computer graphics. *Applied Agricultural Research* **2**(4): 277–289.
- Stephens DB. 1993. A perspective on diffuse natural recharge mechanisms in areas of low precipitation. *Soil Science Society of America Journal* **58**(1): 40–48.
- Stockle CO. 1985. *Simulation of the effect of water and nitrogen stress on growth and yield of spring wheat*. PhD dissertation, Washington State University: Pullman, WA.
- Stoertz MW, Bradbury KR. 1989. Mapping recharge areas using a groundwater flow model—a case study. *Ground Water* **27**(2): 220–229.
- Wang H, Zhang L, Dawes WR, Liu C. 2001. Improving water use efficiency of irrigated crops in the North China Plain—measurement and modelling. *Agricultural Water Management* **48**(2): 151–167.
- Wood WW, Sanford WE. 1995. Chemical and isotopic methods for quantifying groundwater recharge in a regional semiarid environment. *Ground Water* **33**(3): 458–468.
- Xu G, Peel LJ. 1991. *The Agriculture of China*. Oxford University Press: New York; 300 pp.
- Yang S. 1991. The ten agricultural regions of China. In *The Agriculture of China*, Xu G, Peel LJ (eds). Oxford University Press: New York; 108–143.
- Zhang Q, Zhang X. 1995. Water issues and sustainable social development in China. *Water International* **20**(3): 122–128.
- Zhang X. 1999. *Crop Root Growth and Distribution in Soil in the North China Plain*. Meteorological Press: Beijing; 186 pp. (In Chinese.)
- Zhang X, Yuan X. 1994. Analysis of agricultural climatic conditions and water-requirement laws of the major crops: winter wheat and summer maize. In *Eco-Agricultural Experimental Research of the Chinese Academy of Sciences*, Wang S, Zeng J, Lu F (eds). Shijiazhuang Institute of Agricultural Modernization, Luancheng Eco-Agricultural Research Station, China Science and Technology Press: Beijing; 114–119. (In Chinese.)
- Zhang Y, Liu C, Shen Y, Kondoh A, Tang C, Tanaka T, Shimada J. 2002. Measurement of evapotranspiration in a winter wheat field. *Hydrological Processes* **16**(14): 2805–2817.

- Zhu Y, Zheng X. 1983. Shallow groundwater resources of the Huang-Huai-Hai plain. In *Long-distance Water Transfer: a Chinese Case Study and International Experiences*, Chapter 18, Biswas AK, Zuo D, Nickum JE, Liu C (eds); United Nations University. [Accessed 31 October 2000 from URL <http://www.unu.edu/unupress/unupbooks/80157e/>]
- Zollweg JA, Gburek WJ, Steenhuis TS. 1996. SMoRMod—a GIS-integrated rainfall–runoff model applied to a small northeast U.S. watershed. *Transactions American Society of Agricultural Engineers* **39**(4): 1299–1307.